

# Diblock Copolymer Thin Film Melts on Striped, Heterogeneous Surfaces: Parallel, Perpendicular and Mixed Lamellar Morphologies

G. G. Pereira<sup>\*,†,‡</sup> and D. R. M. Williams<sup>†</sup>

Department of Applied Mathematics, Research School of Physical Sciences and Engineering,  
Australian National University, Canberra ACT, 0200, Australia, School of Chemistry,  
University of Sydney, NSW 2006, Australia

Received June 26, 1998

**ABSTRACT:** We consider the problem of a diblock copolymer melt thin film on a striped surface. Because of the different surface energies, the different stripes have different preferences for each of the blocks, while the upper free surface may also prefer one of the blocks. As a result of a combination of factors such as the surface tensions and chain stretching, a number of morphologies may appear. We allow for perpendicular, parallel, and mixed type lamellae and study the resulting phase diagrams. These diagrams should provide a crude guide for experimental studies on such systems. Our main conclusions are 2-fold. First the phase diagram is intricate and complicated. Second, to produce a single crystal oriented along the stripes, it is best to use thin films and a diblock lamellar size equal to or larger than the stripe width.

## 1. Introduction

Diblock copolymers are made up of two chemically different polymer chains, denoted by A and B, joined together end to end. In a bulk melt sample the self-assembly of the diblocks is driven by the immiscibility of the A and B components leading to microphase separation into a variety of morphologies.<sup>1–3</sup> For symmetric diblocks i.e., equal numbers of A and B monomers of the same size, a lamellar phase forms where the system forms a stack of AB–BA bilayers, with average lamellar size  $L_b \approx 1000$  Å. This morphology minimizes the total of the AB interfacial energy and the elastic energy. Studies on thin films of diblock melts<sup>4–12</sup> on homogeneous surfaces have rapidly increased recently in part because of possible applications in surface modification and adhesion. More recently it has become possible to manufacture patterned surfaces, consisting of alternating stripes, with stripe width,  $\lambda$ , comparable to the average lamellar size.<sup>13</sup> If one of the stripes favors the A monomers and the other stripe B monomers, the lamellae should form perpendicular to the surface and be commensurate with the stripes. Such well-defined lamellae may have applications in growing “single crystals” for templating in lithographic processes.<sup>14</sup> Theoretical studies on the morphology of the thin film melt on such patterned surfaces have begun.<sup>14–16</sup> In our previous study, we considered the scenario where the lamellae align perpendicular to the surface as in parts a and b of Figure 1. These we call perpendicular morphologies. We showed that commensurate, incommensurate, or inverted lamellar morphologies may occur. Commensurate morphologies are those whose lamellae are all equal and align precisely with the surface stripes. On the other hand incommensurate lamellae are those where the lamellar size are not all the same. As well, we predicted inverted lamellae in certain local regions of the film where the pattern of the lamellae is not the usual AB, BA but rather AB, AB. In our previous study<sup>15</sup> we assumed the interfacial tensions between the A block and the top (air) surface

and the B block and the top surface were equal. As a result a purely perpendicular morphology should be observed. Of course this assumption is an oversimplification which proved useful in an initial study of this complicated system. In this paper we relax these constraints. We shall allow the A-block–air interfacial energy,  $\gamma_{AF}$ , and the B-block–air interfacial energy,  $\gamma_{BF}$ , to be different. As a result the melt may form a parallel lamellar morphology or indeed a mixed morphology (see Figure 1) with perpendicular orientation near the striped surface and parallel orientation at the upper free surface. Recently there have been a few studies on mixed lamellae on homogeneous surfaces.<sup>17–20</sup> They have been observed experimentally<sup>17</sup> and by Monte Carlo computer simulations,<sup>18</sup> although a theoretical self-consistent mean field study<sup>19</sup> has shown them to be only marginally stable.

Our main aim in this study is to provide a crude guide to what might be seen experimentally when the various parameters such as film thickness and interfacial tensions are varied. Our study in keeping with all other theoretical studies of diblocks, assumes a series of trial geometries for the state of the film. We choose the geometry from our finite set which has the minimum free energy. Of course we cannot guarantee that the actual geometry chosen by nature will be among our finite set and we have to rely somewhat on intuition. We emphasize that our study is meant as a rough guide and is certainly not a definitive or final word on the subject. The system is very rich, and it is unlikely that we have examined all the possible morphologies that will occur. In addition, we ignore fluctuation effects and distortions of the lamellar interfaces. Despite this caveat, the study should be useful, particularly if one wishes to know how to produce single crystals of lamellae orientated along the stripes. We can say definitely where such crystals are not the equilibrium structure and can thus show which regions of the phase diagram should be avoided.

Guided by the experiments<sup>13</sup> we assume in this study that the diblocks are strongly segregated. We specialize to the case of symmetric diblocks, i.e., equal numbers of A and B monomers, denoted by  $N$ , and with the same

<sup>†</sup> Australian National University.

<sup>‡</sup> University of Sydney.

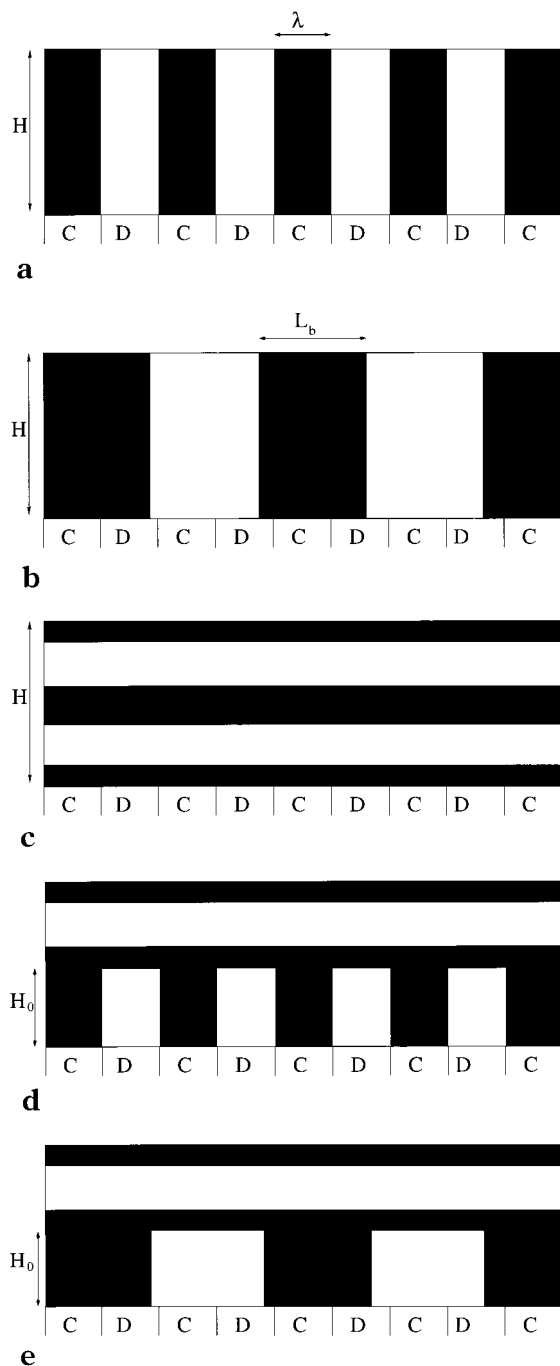


**Figure 1.** Schematic of the side-on view of the diblock melt thin film for the various morphologies. Black represents B lamellae and white represents A lamellae. (a) A surface perpendicular morphology which is commensurate with the CD stripes. (b) A bulk perpendicular morphology which ignores the CD stripes. (c) A parallel morphology. (d) A mixed surface morphology with perpendicular orientation of the diblocks aligned commensurate with the stripes at the bottom of the film and parallel orientation of the lamellae at the top of the film. (e) A mixed bulk morphology with similar structure to the mixed surface morphology except that the perpendicular lamellae have spacing  $L_b$  rather than  $\lambda$ .

monomer size  $a$ . Thus a lamellar phase forms<sup>1-3</sup> with lamellar size  $L_b = [(48\gamma_{AB}a^5)/(\pi^2 k_B T)]^{1/3} N^{2/3}$ , where  $\gamma_{AB}$  is the AB interfacial tension and  $T$  is the temperature. We assume the system minimizes its free energy, although in practice the system may take a considerable time to reach equilibrium. We shall also assume all interfaces remain flat, although it is well-known that systems such as these, which are intrinsically strained,

may form islands and holes<sup>10</sup> or undulate.<sup>12,21</sup> We will leave a study of these undulations to future work.

## 2. Diblock Morphologies

To determine which morphology is favored we first determine the free energies of the various possible morphologies. For definiteness we consider a surface with  $2n$  stripes in total, with  $n$  large (effectively infinite). The stripes are either C or D stripes and alternate, with C stripes preferring B blocks and D stripes preferring A blocks.

**2.1. Perpendicular Surface Morphology.** Initially we consider the purely perpendicular morphologies. In the following all lengths are measured with respect to the stripe width  $\lambda$  and all interfacial tensions are given with respect to the bulk AB interfacial tension,  $\gamma_{AB}$ . When the diblock-stripped surface interfacial energies are sufficiently large the lamellae will be commensurate with the stripes<sup>15</sup> (see Figure 1a). We call this morphology a perpendicular surface morphology and its (dimensionless) free energy averaged over each pair of stripes, per unit length in the direction along the stripes, is given by

$$F_{\text{surf}} = 2H \left( \frac{1}{2L^3} + 1 \right) + g_{AD} + g_{BC} + g_{AF} + g_{BF} \quad (1)$$

where  $H$  is the (dimensionless) film thickness i.e.,  $H = h/\lambda$ , where  $h$  is the actual film thickness.  $L$  is the (dimensionless) lamellar size i.e.,  $L = L_b/\lambda$  and  $g_{ij}$  is the (dimensionless) interfacial tension between an  $i$  block and the  $j$  species (either stripe or air) i.e.,  $g_{ij} = \gamma_{ij}/\gamma_{AB}$ . The first term in the free energy is due to stretching of the diblocks, the second term is the AB interfacial contribution while the other terms are the surface interfacial energy contributions.

**2.2. Perpendicular Bulk Morphology.** The second perpendicular morphology we shall consider is a "bulk" like morphology i.e., a morphology that has the bulk lamellar spacing (Figure 1b). This morphology will form when bulk contributions dominate surface contributions i.e., for thick films and  $L$ 's significantly different from unity. The free energy of the bulklike morphology is

$$F_{\text{bulk}} = \frac{3H}{L} + \frac{g_{AD} + g_{AC} + g_{BD} + g_{BC}}{2} + g_{AF} + g_{BF} \quad (2)$$

In principle there may also exist a large number of incommensurate morphologies,<sup>15</sup> but in the interests of simplicity we shall neglect them here. However we shall have something to say about these incommensurate morphologies near the end of the paper. Note that perpendicular morphologies may also form on homogeneous surfaces when the film thickness is significantly different from  $L_b$ .<sup>11</sup>

**2.3. Parallel Morphology.** The next case we consider is a parallel morphology. In this case the lamellae are parallel to the surface (Figure 1c). Such a morphology should form if one of the blocks is preferred, to a significant extent, at either top (air) or bottom surfaces. As mentioned before, in general,  $g_{AF}$  and  $g_{BF}$  are unequal so that one block may be preferred at the top surface. As well, even though we assume C stripes prefer B blocks and D stripes prefer A blocks there may still be an overall preference for either block at the striped surface. In general the thickness of the film is not an integer multiple of  $L_b$ , and so the number of

lamellae in the parallel morphology has to be minimized between a configuration with  $q$  lamellae or  $q + 1$  lamellae.<sup>4</sup> Here  $q$  is the greatest integer less than or equal to  $H/L$ . The free energy of the parallel morphology is thus

$$F_{\text{parallel}} = 2 \left( \frac{H^3}{2q^2L^3} + q \right) + g_{\text{ID}} + g_{\text{IC}} + 2g_{\text{IF}} \quad (3)$$

where  $i$  and  $j$  can be either A or B blocks.

**2.4. Mixed Surface Morphology.** We also consider the mixed surface morphology. This morphology should exist when there is strong alignment of the perpendicular orientation near the striped surface and strong alignment of the parallel orientation at the top surface. The cost in energy is extra AB interfacial area at the junction between perpendicular and parallel lamellae (Figure 1d). The free energy of a mixed morphology, with commensurate alignment of the lamellae at the bottom surface, is given by

$$F_{\text{MS}} = 2H_0 \left( \frac{1}{2L^3} + 1 \right) + 2 \left[ \frac{(H - H_0)^3}{2q^2L^3} + q \right] + 1 + g_{\text{AD}} + g_{\text{BC}} + 2g_{\text{IF}} \quad (4)$$

where  $H_0$  is the thickness of the perpendicular part and  $q$  is the greatest integer less than or equal to  $(H - H_0)/L$ . We assume in this paper that the interface between the parallel and perpendicular sections of the sample is sharp. In principle the system can create a smoother crossover between these two geometries<sup>22,23</sup> and our estimate of the free energy is thus only an upper bound.

**2.5. Mixed Bulk Morphology.** Another mixed state that may exist is one where the perpendicular alignment at the bottom has bulk spacing (Figure 1e). The free energy of such a morphology is

$$F_{\text{MB}} = \frac{3H_0}{L} + 2 \left[ \frac{(H - H_0)^3}{2q^2L^3} + q \right] + 1 + \frac{g_{\text{AC}} + g_{\text{AD}} + g_{\text{BC}} + g_{\text{BD}}}{2} + 2g_{\text{IF}} \quad (5)$$

The above expressions for the free energy of the mixed lamellar morphologies must be minimized over  $H_0$ , where clearly  $0 < H_0 < H$ , and  $q$ , just as in the parallel case. It is now our task to compare the free energies of these five possible morphologies to determine which morphology exists. The free energy differences are functions of  $H$ ,  $L$ ,  $g_{\text{C}} \equiv g_{\text{AC}} - g_{\text{BC}} \geq 0$ ,  $g_{\text{D}} \equiv g_{\text{BD}} - g_{\text{AD}} \geq 0$  and  $g_{\text{F}} \equiv g_{\text{AF}} - g_{\text{BF}}$  and so the phase diagram depends on five free parameters. In the present study we have assumed all interfaces are sharp and flat. These assumptions should hold on a qualitative level in the strong-segregation limit. However these interfaces are probably much more irregular or distorted. Although including the effect of such distortions is beyond the scope of the present study, from some recent preliminary calculations of ours it would appear such distortions do not have a significant effect on the (qualitative) phase diagrams we calculate.

### 3. Results and Discussion

Initially we assume that there is no overall preference at the bottom surface, so  $g_{\text{C}} = g_{\text{D}}$ , and we are left with four free parameters. Our results are given in the form

of  $g_{\text{F}}$  vs  $H$  phase diagrams, for given  $L$  and  $g_{\text{C}}$ . These results are typical of all the results we obtained. Consider Figure 2 which is calculated for  $L = 1.5$  and various values of  $g_{\text{C}}$ . For  $L = 1.5$  the lamellae are compressed if they align exactly with the stripes. Note that the phase diagram is symmetric about  $g_{\text{F}} = 0$  and so we only show the half  $g_{\text{F}} \leq 0$ . This corresponds to A-blocks being preferred overall at the air-copolymer interface. For  $g_{\text{F}}$  close to zero and  $H$  small, we see that the purely perpendicular morphologies exist (Figure 1a, dark gray shading, and Figure 1b, black shading). For small film thicknesses the diblock-stripe potential is dominant and the whole film aligns commensurate with the stripes. At some critical thickness  $H_{\text{c}}$  there is a transition to a bulk, perpendicular morphology (Figure 1b, black shading). It can be shown that for any  $L$  and  $g_{\text{F}}$  this critical thickness is given by  $H_{\text{c}} = L^3(g_{\text{C}} + g_{\text{D}})/[2(2L^3 - 3L^2 + 1)]$ , so that for  $L = 1.5$ ,  $H_{\text{c}} \approx 3.375$ . Note that in Figure 2a the parallel morphology (Figure 1c, white shading) actually appears for  $g_{\text{F}} = 0$  in the neighborhood of  $H = 4.5, 6, 7.5, 9, \dots$ , because in these regions the parallel lamellae have a spacing close to  $L_{\text{b}}$ . For  $|g_{\text{F}}| \gg 0$ , we find that the interfacial energy at the top surface becomes important. As a result either parallel (Figure 1c, white shading) or mixed morphologies (Figure 1d,e) may occur. Consider the possible morphologies for  $g_{\text{F}} = -2.0$ . For very small thicknesses we still obtain a purely perpendicular surface morphology (Figure 1a, dark gray shading) with lamellae commensurate with surface stripes. As  $H$  gets larger we have a transition to a parallel morphology (Figure 1c, white shading). This parallel morphology has only one lamella in the pattern BA. Since  $H$  is small in this region, i.e., less than unity, one lamella is the optimum number of lamellae which minimizes the free energy of the diblocks. As  $H$  increases we obtain a transition to a mixed surface lamellar morphology (Figure 1d, light gray shading), with lamellae aligned with the stripes at the bottom of the film and parallel orientation at the top of the film. The number of parallel lamellae in this mixed state is one i.e., a BA lamella. As  $H$  increases, the thickness of the perpendicular part of the mixed state, i.e.,  $H_0$ , also increases. Further increase in  $H$  results in a transition back to a purely parallel morphology, but now with two lamellae in the pattern AB, BA. This scenario, of alternating between mixed and parallel morphologies, continues as  $H$  increases. However as  $H$  increases the size of the mixed region decreases, until, for thick films, we only obtain parallel morphologies. Note we never observe a mixed bulk morphology (Figure 1e). The mixed bulk morphology would be expected to occur in those parts of the phase diagram where the parallel morphology exists. However the extra interfacial energy that results at the junction between perpendicular and parallel regions is presumably too large, compared to the free energy of a purely parallel state. Note that as  $g_{\text{C}}$  increases the region of mixed surface morphology becomes much larger; i.e., the effect of the striped surface becomes much more important.

An interesting question that Figure 2 poses is why do the mixed morphologies appear between parallel morphologies. We can understand this as follows. For small  $g_{\text{C}}$ , the surface has negligible effect and so, for sufficiently large  $|g_{\text{F}}|$ , the lamellae will align independently of the striped surface i.e., in a parallel morphol-



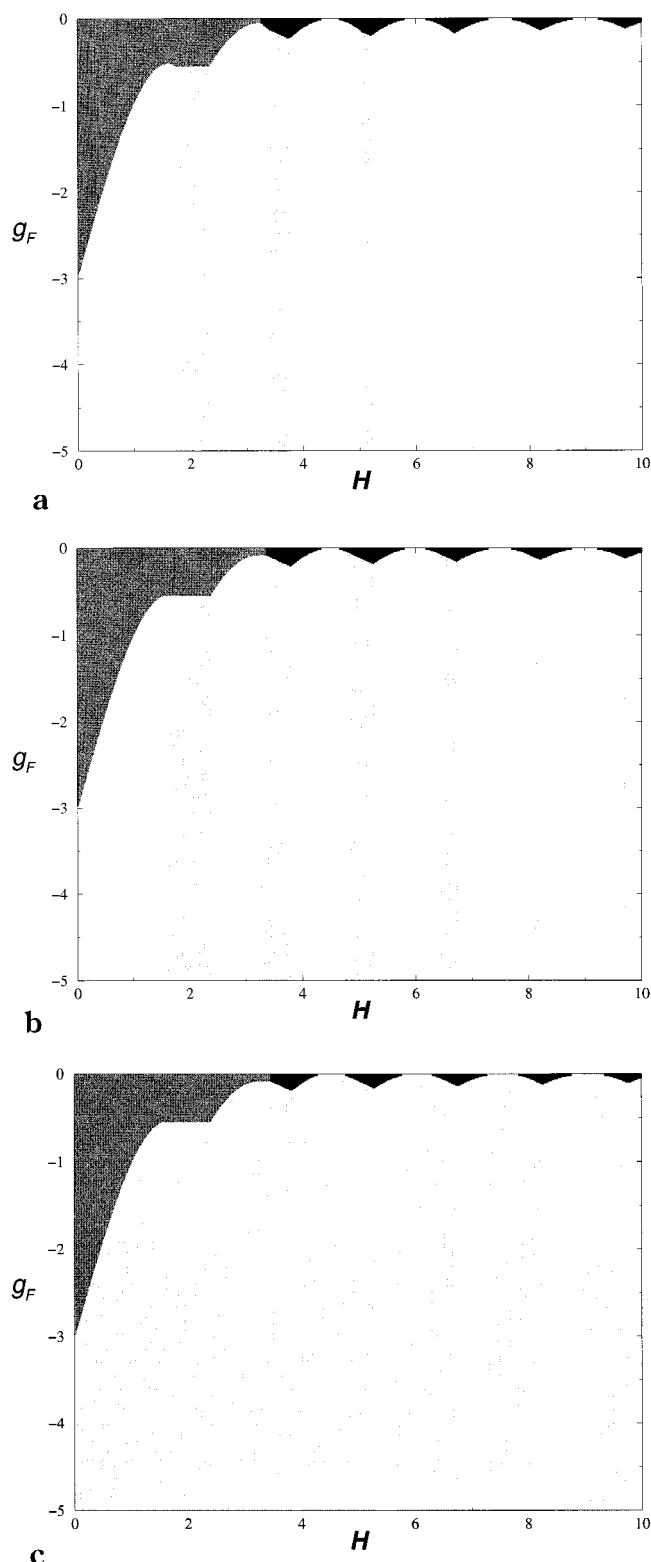
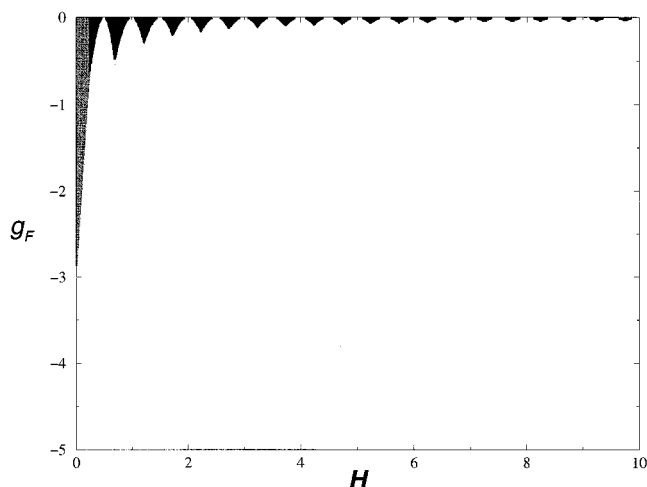


**Figure 2.** Phase diagram in the  $H$ - $g_F$  plane for  $L = 1.5$  and  $g_C = g_D$ : (a)  $g_C = 0.97$ ; (b)  $g_C = 1.0$ ; (c)  $g_C = 1.03$ . The black region represents bulk morphology, the white region represents parallel morphology, the dark gray region is surface morphology, and the light gray is mixed surface morphology. Note, in this and the following phase diagrams, we have chosen  $g_C$  close to unity because this implies all the surface tensions are roughly comparable and so all phases appear in the phase diagram. For example we have investigated the phase diagram for  $g_C = 1.5$  and we find the mixed surface morphology takes over the entire parallel region in Figure 2c.

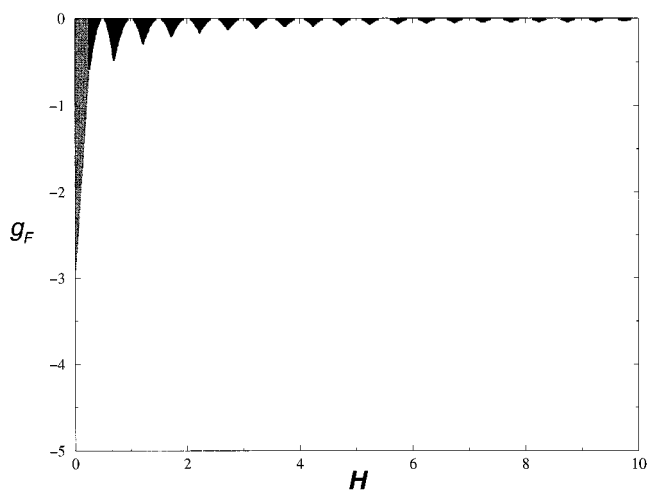
ogy. The parallel state has minimum free energy when the film thickness is an integer multiple of  $L_b$  i.e., in

this case  $H = 1.5, 3, 4.5, \dots$ . A transition from  $m$  to  $m + 1$  lamellae, where  $m = 1, 2, \dots$ , occurs roughly midway between these points, i.e., at  $2.25, 3.75, \dots$ , and the free energy of these two possible states is the maximum free energy in the interval  $H = (m - 1/2)L$  to  $(m + 1/2)L$ . Thus it is at these points where any new morphology will appear first. These are precisely the points at which the mixed surface morphologies first appear. Note that a more accurate estimation of the transition thickness from  $m$  to  $m + 1$  layers can be made by equating these two states' free energies, as carried out by Turner,<sup>4</sup> but it is not required for the present discussion. Next we consider the case where  $L = 0.5$  (Figure 3). This is different to the previous case since now the lamellae actually have to stretch if they are to have a spacing of  $\lambda$ . In contrast to the case where  $L > 1$ , the stretching energy thus increases if a perpendicular surface morphology forms. The overall free energy must therefore increase since the number of AB interfaces is constant for the perpendicular surface morphology. For  $g_F$  close to zero, we again see purely perpendicular morphologies, but note now the critical thickness at which there is a transition from the perpendicular surface morphology (Figure 1a, dark gray shading) to the perpendicular bulklike morphology (Figure 1b, black shading) is  $H_c \approx 0.25$ . This is much smaller than in Figure 2 and can be attributed to the much larger stretching the diblocks must undergo. The overall structure of the phase diagram is similar to that in Figure 2. The most notable difference is that the parallel morphology (Figure 1c, white shading) exists over a much larger part of the phase diagram. Thus we see that the striped surface has a much greater effect on melts with bulk equilibrium spacing  $L_b > \lambda$  than for melts with  $L_b < \lambda$ , because of the different stretching scenarios i.e., for the former case the diblocks are compressed when in the surface morphology, while in the latter case the diblocks are stretched and so lose energy. Once again we never observe the mixed bulk morphology (Figure 1e).

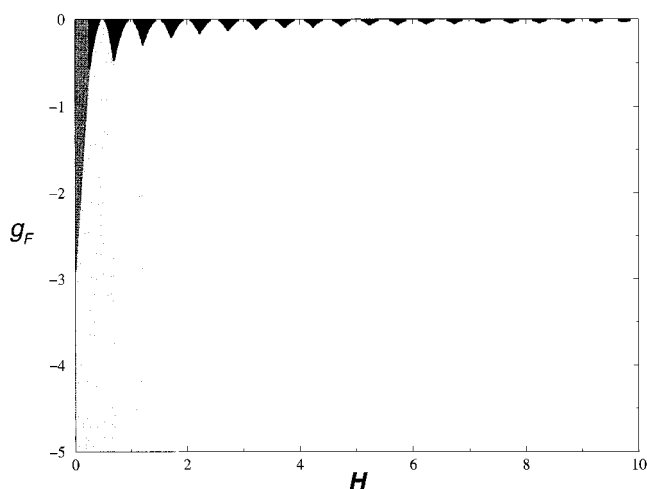
In Figure 4 we display the result for  $L = 1.0$  and various  $g_C$ . Since the lamellar size and stripe width are exactly the same the perpendicular surface morphology (Figure 1a, dark gray shading) exists for all thicknesses for sufficiently small  $|g_F|$ , i.e.,  $|g_F| < 1$ . For larger  $|g_F|$  and  $g_C = 1.0$  the mixed surface morphology (Figure 1d, light gray shading) exists everywhere except for very thin films i.e.,  $H < 1$ . For large  $|g_F|$ , the air-copolymer surface tension makes the lamellae align parallel near the top of the film, while near the bottom of the film, there can be perpendicular alignment of the lamellae. For  $H < 1$  the film is too thin for a mixed morphology to fit and so only a parallel morphology (Figure 1c, white shading) exists. However as  $g_C$  becomes larger the striped surface-diblock energy increases and so the parallel morphology region decreases in size, in fact disappearing from the phase diagram for  $g_C = 1.03$ . Thus far we have examined the case  $g_C = g_D$  where there is no overall preference for either diblock at the surface. We now briefly consider the case  $g_C \neq g_D$ . Doing this means the system should become biased toward parallel morphologies since now one block is favored overall at the striped surface. Consider Figure 5a which is calculated for  $g_C = 0.5$ ,  $g_D = 1.0$  and  $L = 1.5$ . This implies the A-blocks are favored overall at the bottom surface. Figure 5a shows that the phase diagram is now not symmetrical about  $g_F = 0$  and also the parallel morphology (Figure 1c, white shading) takes up a much



a



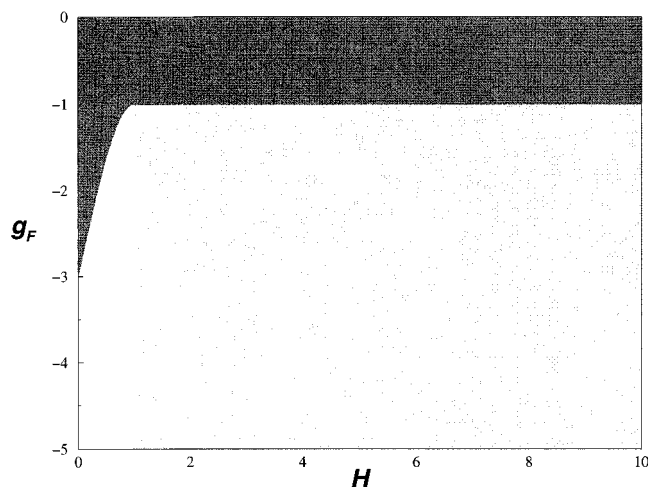
b



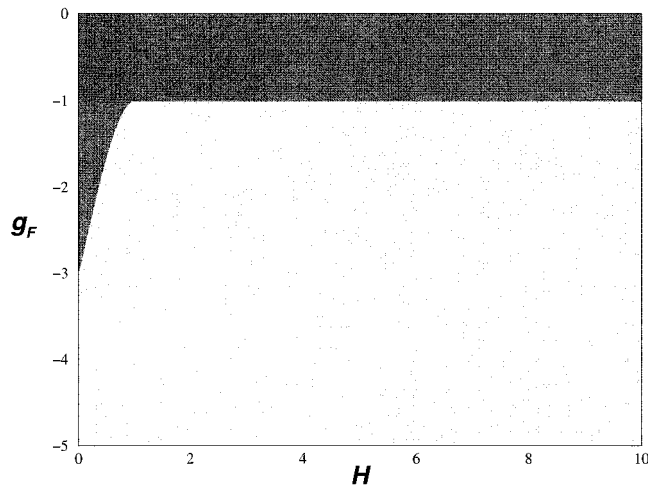
c

**Figure 3.** Phase diagram in the  $H$ - $g_F$  plane for  $L = 0.5$  and  $g_C = g_D$ : (a)  $g_C = 0.97$ ; (b)  $g_C = 1.0$ ; (c)  $g_C = 1.03$ . The same shading scheme, for the various morphologies, as in Figure 2 applies here.

larger region. For  $g_F < 0$ , A blocks are favored at both upper and lower surfaces. Thus the AB, BA parallel pattern for  $1.5 < H < 2.5$  takes up a larger region of the phase diagram (cf., Figure 2b); i.e., it "eats" into perpendicular and mixed morphology regions. On the other hand, the region corresponding to the BA parallel pattern (i.e.,  $H < 1.5$ ) does not increase in size. In the



a



b

**Figure 4.** Phase diagram in the  $H$ - $g_F$  plane for  $L = 1.0$  and  $g_C = g_D$ : (a)  $g_C = 1.0$ ; (b)  $g_C = 1.03$ . The same shading scheme, for the various morphologies, as in Figure 2 applies here.

region  $2.5 < H < 3.5$  the BA, AB, BA parallel pattern takes up a smaller region of the phase diagram, while the AB, BA, AB parallel pattern from  $g_F > 0$  pushes into the  $g_F < 0$  region. As a result the region corresponding to the perpendicular bulk morphology (Figure 1b, black shading) also diminishes in size. In Figure 5b, we show the phase diagram for  $L = 1.0$  and  $g_C = 0.5$  and  $g_D = 1.0$ . Once again the diagram is asymmetric with the perpendicular surface morphology (Figure 1a, dark gray shading) existing for small  $g_F$  and all thicknesses. Compared with Figure 4a, we again see the parallel morphology (Figure 1c, white shading) region increases in size since now the lower surface prefers the A blocks overall.

#### 4. Conclusions

In this paper, we have set out to determine the possible lamellar morphologies that can appear when a thin film diblock copolymer melt is placed on a striped heterogeneous surface. Although we have chosen the possible morphological structures, we believe these to be intuitively reasonable. One obvious conclusion is that the phase diagram for these systems is intricate and complicated with many re-entrant regions. When there is negligible overall preference between the blocks at the striped surface we find the perpendicular morphol-

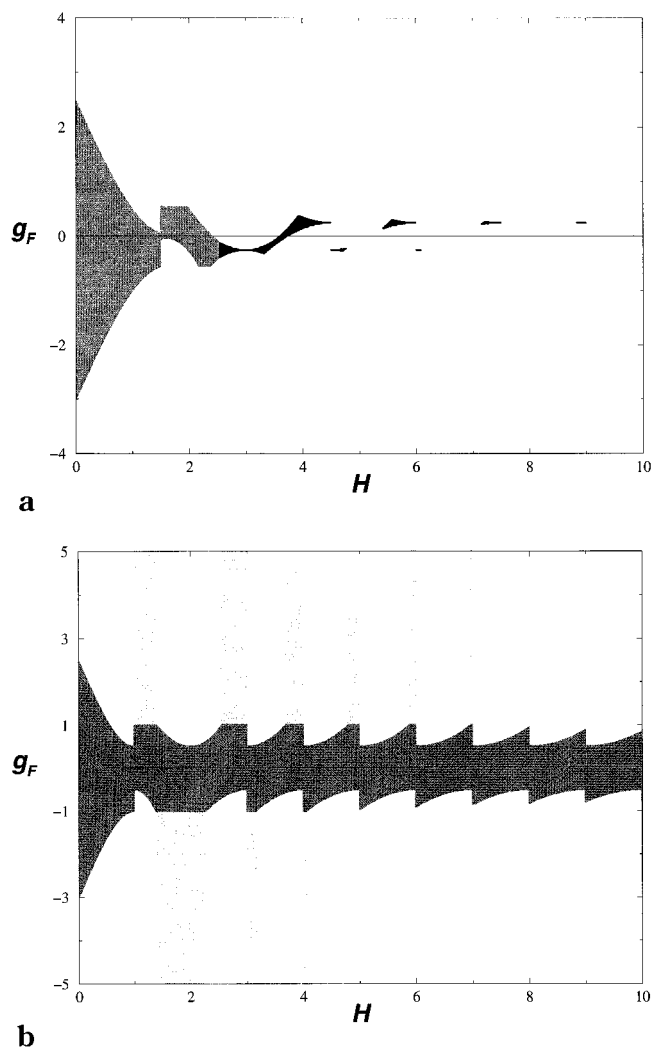


**Figure 5.** Phase diagram in the  $H$ - $g_F$  plane for (a)  $L = 1.5$ ,  $g_C = 0.5$ , and  $g_D = 1.0$  and (b)  $L = 1.0$ ,  $g_C = 0.5$ , and  $g_D = 1.0$ . The same shading scheme, for the various morphologies, as in Figure 2 applies here.

ogies can take up a large portion of the phase diagram. For  $g_F$  very close to zero and small film thicknesses, we find purely perpendicular morphologies, in agreement with our previous study.<sup>15</sup> However as  $|g_F|$  becomes larger we find both parallel orientation of the lamellae and a mixed type morphology, where, near the striped surface, there are perpendicular lamellae commensurate with the stripes and, at the top of the film, parallel lamellae. This morphology attempts to minimize the (exterior) surface interfacial energies but, as a result, introduces extra (interior) AB interfacial energy. When there is a significant overall preference for one of the blocks at the striped surface we find the parallel morphologies take up increasingly larger portions of the phase diagram.

Recently there have been two numerical (Cahn–Hilliard) mean-field studies on the morphologies of diblock melts on striped surfaces. Petera and Muthukumar<sup>14</sup> concentrate primarily on melts in the weak-segregation limit. The effect of the striped surface is then to enhance microphase separation of the A and B blocks into lamellae perpendicular and commensurate with the striped surface. Chen and Chakrabarti<sup>16</sup> focus, like us, on the strong-segregation limit, but restrict themselves to  $L_b \leq \lambda$  and the case where the interfacial tensions between air and the blocks are the same. They

find alignment of the lamellae with the stripes when  $L_b \approx \lambda$ , but when  $L_b \approx \lambda/2$  they find that the lamellae may be commensurate with the stripes or completely ignore the stripes depending on film thickness. They also find for some thicknesses a mixed morphology (similar to our mixed morphology). Our study should be seen as a generalization of Chen and Chakrabarti's study<sup>16</sup> in the sense that we can give a qualitative answer as to the possible lamellar morphology for given thickness and interfacial tensions. Chen and Chakrabarti's study only considers a few points in the entire phase diagram.

In our previous study we also predicted incommensurate and inverted lamellae.<sup>15</sup> For simplicity we have not included the presence of such lamellae in this study but we can say something about their existence. Certainly for  $g_F = 0$ , our present study implies that these types of morphologies will appear and may be observed experimentally either from an overhead view or a side-on view (i.e., similar to the views shown in the schematics in Figure 1). For  $g_F \neq 0$ , we believe incommensurate or inverted lamellae will still occur in the perpendicular part of the mixed morphology. Our reasoning for this is as follows. It was shown previously<sup>15</sup> that incommensurate, or inverted, lamellae may indeed be the minimum free energy configuration for certain values of the parameters—thickness, bulk lamellar size, and interfacial tensions. Since at the junction between mixed and parallel lamellae the amount of AB interfacial area is a constant, i.e., independent of the exact morphology of the perpendicular lamellae underneath, incommensurate and inverted lamellae may still be the minimum free energy configuration in the perpendicular part. As a result, although from an overhead view these incommensurate lamellae will not be seen, from a side-on view they will be seen at the bottom of the film.

On a more practical point if one wants to grow a “single crystal” of the lamellar phase, with lamellar size  $\lambda$ , it is better to have  $L_b > \lambda$  than  $L_b < \lambda$ , since in the former case the region taken up by the perpendicular surface morphology in the phase diagram is much larger than in the latter case. As well it would be beneficial to have a negligible difference between preference for the two blocks at the top and bottom interfaces.

**Acknowledgment.** G.G.P. and D.R.M.W. acknowledge support from an ARC Large Grant and D.R.M.W. is supported by an ARC QEII.

## References and Notes

- (1) Bates, F. S.; Fredrickson, G. H. *Annu. Rev. Phys. Chem.* **1990**, *41*, 525.
- (2) Helfand, R.; Wasserman, Z. R. *Macromolecules* **1976**, *9*, 879.
- (3) Semenov, A. N. *Sov. Phys.—JETP (Engl. Transl.)* **1985**, *61*, 733 [*Zh. Eksp. Teor. Fiz.* **1985**, *88*, 1242].
- (4) Turner, M. S. *Phys. Rev. Lett.* **1992**, *69*, 1788.
- (5) Turner, M. S.; Joanny, J.-F. *Macromolecules* **1992**, *25*, 6681.
- (6) Kellogg, G. J.; Walton, D. G.; Mayes, A. M.; Lambooy, P.; Gallagher, P. D.; Satija, S. K. *Phys. Rev. Lett.* **1996**, *76*, 2503.
- (7) Walton, D. G.; Kellogg, G. J.; Mayes, A. M.; Lambooy, P.; Russell, T. P. *Macromolecules* **1994**, *27*, 6225.
- (8) Coulon, G.; Collin, B.; Ausserre, D.; Chatenay, D.; Russell, T. P. *J. Phys. (Fr.)* **1990**, *51*, 2801.
- (9) Pickett, G. T.; Balazs, A. C. *Macromolecules* **1997**, *30*, 3097.
- (10) Halperin, A.; Sommer, J. U.; Daoud, M. *Europhys. Lett.* **1995**, *29*, 297.
- (11) Heier, J.; Kramer, E. J.; Walheim, S.; Krausch, G. *Macromolecules* **1997**, *30*, 6610.
- (12) Walton, D. G.; Kellogg, G. J.; Mayes, A. M.; Lambooy, P.; Russell, T. P. *Macromolecules* **1994**, *27*, 6225.
- (13) Williams, D. R. M. *Phys. Rev. Lett.* **1995**, *75*, 453.

- (13) Liu, Y.; Rockford, L.; Russell, T. P.; Mansky, P.; Soong, S.; Yoon, M.; Mochrie, S. Submitted for publication in to *Phys. Rev. Lett.* Presentation at MRS Fall Symposium, Boston, MA, 1997. Presentation at APS Meeting, Los Angeles, CA, 1998. Falsolka, M. J.; Harris, D. J.; Mayes, A. M.; Yoon, M.; Mochrie, S. G. *J. Phys. Rev. Lett.* **1997**, *79*, 3018.
- (14) Petera, D.; Muthukumar, M. *J. Chem. Phys.* **1997**, *107*, 9640.
- (15) Pereira, G. G.; Williams, D. R. M. *Macromolecules* **1998**, *31*, 5904. *Phys. Rev. Lett.* **1998**, *80*, 2849.
- (16) Chen, H.; Chakrabarti, A. *J. Chem. Phys.* **1998**, *108*, 6897.
- (17) Koneripalli, N.; Levicky, R.; Bates, F. S.; Ankner, J.; Kaiser, H.; Satija, S. K. *Langmuir* **1996**, *12*, 6681. Mansky, P.; Russell, T. P.; Hawker, C. J.; Pitsakalis, M.; Mays, J. *Macromolecules* **1997**, *30*, 6810.
- (18) Kikuchi, M.; Binder, K. *J. Chem. Phys.* **1994**, *101*, 3367.
- (19) Matsen, M. W. *J. Chem. Phys.* **1997**, *106*, 7781.
- (20) Tang, W. H.; Witten, T. A. *Macromolecules* **1998**, *31*, 3130.
- (21) Helfrich, W. *Appl. Phys. Lett.* **1970**, *17*, 531. Hurault, J. P. *J. Chem. Phys.* **1973**, *59*, 2068.
- (22) Netz, R. R.; Andelman, D.; Schick, M. *Phys. Rev. Lett.* **1997**, *79*, 1058.
- (23) Gido, S. P.; Thomas, E. L. *Macromolecules* **1994**, *27*, 6137.

MA981003N